

Advanced Solar Imaging from the GOES R Spacecraft

Steven M. Hill and Victor J. Pizzo
NOAA Space Environment Center, Boulder, Colorado

ABSTRACT

The NOAA Space Environment Center is proposing enhanced real-time solar observations to be conducted aboard the GOES satellites in the next decade. These spacecraft are in geosynchronous orbit and offer a convenient platform for near-continuous, high data rate monitoring of the Sun and the interplanetary environment. The instrument complement being considered includes at least two solar imagers: 1) an advanced soft X-ray telescope featuring selectable spectral bandpass, large dynamic range, and high image cadence; and 2) a white light coronagraph with moderate resolution and a field of view sufficient to capture events of geophysical significance. Used in combination with other observational assets, this instrumentation would make a significant improvement in space weather forecast capabilities.

Keywords: Solar Corona, X-ray Imaging, Coronagraph, Space Weather

1. INTRODUCTION

Space weather affects a broad range of technological endeavors on a daily basis. For instance, power companies (independent system operators) limit transmission capacity and generation based on geomagnetic activity and airlines must consider air crew radiation dosage on polar routes from the U.S. to the Far East. The charge of NOAA's Space Environment Center (SEC) is to operationally specify and forecast space environment conditions. Since all space weather originates with the Sun, this is a primary objective of our observations. Note that there are clear differences between NOAA's observational requirements and those of a research oriented instrument. Whereas researchers may seek to 'push the envelope' on instrument resolution or sensitivity, NOAA values reliability and continuity of coverage in its operational systems. NOAA's Geosynchronous Operational Environmental Satellite (GOES) program has included space environment measurements since its inception about a quarter-century ago, beginning with the launch of the Synchronous Meteorological Satellites SMS-1 in 1974. These measurements have provided a consistent historical record and have grown in importance as the Nation's reliance on space and ground-based technology affected by the space environment accelerates. GOES R will continue to support these measurement needs with its launch currently planned for around 2012.

The NOAA Space Weather Scales describe three classes of space weather effects at Earth: Geomagnetic storms, solar radiation storms, and radio blackouts. Technologies affected by geomagnetic storms include terrestrial power transmission grids and spacecraft attitude control systems. Solar radiation storms increase the radiation dose to astronauts and high-latitude/high-altitude air crews and affect spacecraft electronics. Radio blackouts result from 'short-wave fade' as the ionosphere responds to solar X-ray radiation.

Behind each of these impacts is a solar driver. Geomagnetic storms can be initiated by one of two solar sources. Coronal holes, long-lived, large areas of open magnetic field in the solar atmosphere, are the sources of high speed solar wind that can drive recurring geomagnetic storms. The largest geomagnetic storms occur when a coronal mass ejection (CME) from the Sun throws into the interplanetary medium billions of tons of plasma which envelops Earth's magnetic field. Solar radiation storms originate either in direct association with solar flares or with shocks associated with CMEs. Radio blackouts occur in direct response to the enhanced X-ray radiation from solar flares. Increased satellite drag is associated with longer term increases in solar EUV flux. These solar drivers lead to specific high-level operational goals for NOAA observations:

- Locate coronal holes for forecasts of recurring geomagnetic activity
- Locate flares for forecasts of solar energetic particle events
- Assess active region complexity for flare forecasts
- Monitor active regions beyond the east limb for solar activity ($F_{10.7}$) forecasts, and
- Determine occurrence, *speed*, *direction*, and *spatial extent* of coronal mass ejections

The italicized text in the final goal represents the specific improvement that the addition of a white light coronagraph will provide when used in combination with a soft X-ray imager (SXI).

This paper provides insight into the solar imaging instruments under consideration for NOAA’s GOES R spacecraft and the process that sets their requirements. First, the methodology used to set requirements is discussed. Second, current instrument concepts are presented. Third, future plans for instrument development are sketched. Finally, the paper is summarized and conclusions are drawn.

2. REQUIREMENTS

NOAA, NASA, the operational and research communities, and our U.S. Air Force partners are working together to define the requirements for operational solar imagers on the GOES R spacecraft. The relatively clear and long-standing identification of the chief solar signatures of space weather events is discussed first in this section. A discussion of the GOES R requirement process and its current status is then presented. Next, specific observational requirements for the follow-on to the current (GOES 12 and GOES N/O) SXI are described. Finally, observational requirements for a new GOES solar instrument, a white light coronagraph, are outlined.

2.1 Solar Space Weather Signatures

To observe and identify the types of solar activity listed in the high-level operational goals, observables must be quantified. Table 1 provides this information for key signatures of potentially geoeffective solar activity and features. The typical temperature range, and column emission measure (line-of-sight integral of electron density squared) are given for each type of feature. An isothermal spectrum¹ is convolved with a bandpass of 0.6-6.0 nm to give the flux at Earth. The temporal and spatial scales of the features are also listed. Each feature type is discussed in the subsections that follow.

Table 1: Solar Signature Summary in Soft X-rays

Feature	Temperature (MK)	Log EM (cm ⁻⁵)	Flux at Earth (ph-cm ⁻² -arcsec ⁻¹ -sec ⁻¹)	Temporal Scale	Spatial Scale
Coronal Holes	0.9-2.4	25.5-27.0	0.3-26	Weeks to Months	0.05-0.5 R _{SUN}
Flares	7-20	30-32	19,000-1,000,000	Seconds to Hours	10-200 arcsec
Active Regions	2-3	28-29	230-2,800	Weeks to Months	0.05-0.2 R _{SUN}
Solar Activity	0.9-3.0	26-29	1.0-2,800	Hours to Days	0.05-0.2 R _{SUN}
CMEs					
PF Arcades	7-20	30-32	19,000-1,000,000	Minutes to Hours	0.1-0.2 R _{SUN}
Other Transients*	-	-	-	Seconds to Minutes	0.1-0.5 R _{SUN}

*Transients include ‘ejecta’, waves, and dimmings. They have a wide range of temperatures, emission measures, and temporal scales.

2.1.2 Coronal Holes

Coronal holes are seen in a number of spectral bands. In the X-ray and EUV they are seen as regions of substantially decreased emission. In He I 1083 nm they are seen as enhanced emission. Since the corona is optically thin and has substantial vertical extent, unambiguous identification of coronal hole boundaries is complicated by viewing geometry. This might be mitigated by rotational stereoscopy²⁻⁴. Coronal holes exhibit line-of-sight effective temperatures of 0.9-2.4 MK with column emission measures of 10^{23.5}-10²⁷ cm⁻⁵ [refs. 5-7]. While the GOES-N SXI exceeds sensitivity requirements, it still requires exposures of several seconds to achieve SNR~3 for the *dimpest* portions of coronal holes. Thus, while an estimate of the coronal hole boundary can be made, a quantitative measure of conditions in the coronal hole is challenging. However, these conditions are important because they have an influence on both the ion charge states and the speed of the solar wind⁸.

2.1.3 Flares

Along with CMEs, solar flares are among the most energetic solar phenomena and exhibit signatures at all wavelengths. However, the contrast with the pre-flare solar emission is greatest in X-rays. The X-ray emission during the impulsive

phase of a flare comes from a relatively small region and shows substantially elevated temperatures. It also often shows distinct morphologies, e.g., arcade structure. Flares exhibit temperatures of 7-20 MK with emission measures of 10^{30} - 10^{32} cm⁻⁵ [refs. 9, 10]. The greatest challenge in imaging flares is their dynamic range. In soft X-rays, this can exceed 10^5 above local solar background. Thus, it is difficult to image the solar background and simultaneously provide a properly exposed flare image.

2.1.4 Active Region complexity

The ability to forecast flares based on active region properties is currently an empirical art. There is extensive experience in performing such evaluations using white light and H-alpha images as well as using magnetograph data. The state of the art is less mature for X-ray and EUV data, mostly because of the shorter period of experience with such imagery. However, we have seen enough of these images to suggest their usefulness for forecasting. Particularly, loop arcades that have sheared magnetic fields have stored energy available for release¹¹. Similarly, the twisted forms that make up the so-called sigmoidal soft X-ray loops have extra free energy for flaring. Indeed, statistical studies indicate that these configurations are more likely to flare than other configurations¹². Active regions exhibit temperatures of 2-3 MK with emission measures of 10^{28} - 10^{29} cm⁻⁵ [refs. 10, 13, 14].

In addition, there is evidence of pre-flaring signatures, at least in some flares. In X-rays, small brightenings are sometimes seen before the main flare event. In H-alpha and other chromospheric bands, filament motion sometimes precedes flaring.

2.1.5 Solar Activity

Observed solar activity varies with the 27-day rotation period of the Sun as persistent active regions rotate into and out of view. Active regions continue to appear, evolve, and disappear while on the backside of the Sun, so that persistence alone is insufficient to accurately estimate upcoming solar activity levels. However, since the corona is optically thin and has substantial height, it is possible to see beyond the limb in X-rays. Thus, brightness levels above the east limb provide advance estimates of the intensity of active regions rotating onto the front side of the solar disk.

2.1.6 Coronal Mass Ejections

In addition to causing some of the most dramatic space weather effects, coronal mass ejections offer some of the most visually dramatic views of the Sun. As a forecaster, the challenge is to clearly identify and quantify CME signatures at the Sun. Quantification of these signatures can give 1-3 day warning of impending geomagnetic storms. Signatures of CME activity seen in X-rays include: flares, dimmings, post-flare arcades, waves, and filament or filament channel activity. These signatures represent a wide variety of intensities and changes in intensity. For example, while a post-flare arcade could have an emission measure of up to 10^{32} cm⁻⁵, a coronal dimming (mass depletion) could be marked by a decrease in emission measure from $10^{28.5}$ to $10^{28.0}$ cm⁻⁵ at the site of the coronal eruption^{15, 16}.

With a white light coronagraph, CMEs are seen directly via Thomson scattering. The classic three-part CME consists of a bright front, a cavity bounded by that front, and a bright core contained within the cavity. These features can be tracked to obtain plane-of-sky position and speed. Coupled with knowledge of the CME's on-disk point of origin, from soft X-ray images, a three-dimensional trajectory can be roughly inferred. This combination of information is key to forecasting both the magnitude and timing of the most severe geomagnetic storms. The coronal background brightness (F+K corona) ranges from $\sim 10^{-8}$ times the on-disk brightness of the Sun (B_{SUN}) at 2 solar radii (R_{SUN}) to about $10^{-11} B_{\text{SUN}}$ at 30 R_{SUN} . The fractional increase in brightness of a CME compared to the local quiet corona can range from a few to roughly 100 percent from 2 to 5 R_{SUN} ¹⁷. With the F-corona subtracted, the fractional increase over the background K-corona has been observed to be as much as a factor of three¹⁸ at 3.5 R_{SUN} . CME plane-of-sky speeds range from ~ 100 km-s⁻¹ to over 2000 km-s⁻¹ [ref. 19].

2.2 GOES R Requirements Process

There are several threads to developing solar imaging requirements for the GOES R spacecraft. Particularly, there is the determination of the observational requirements for the forecasters to perform their jobs to meet user needs. There is also the need for technical evaluations of instrument concepts to verify that the observational requirements can be met. The GOES R requirement process fulfills both of these needs.

In 2000, NOAA’s Space Environment Center (SEC) began the process of planning for future solar imaging instruments on the GOES spacecraft. A preliminary version of the Operational Requirements Document²⁰ (ORD) was developed in a format consistent with the National Weather Service ORD for tropospheric weather. The SEC document covered observational requirements, as opposed to instrument and engineering specifications, for the Space Environment Monitor instrument suite on GOES. This suite includes *in situ* measurements such as magnetic field and particles as well as remote measurements, such as disk-integrated solar X-ray flux and solar X-ray images. In addition, a number of new measurements were recommended for study.

In October 2001, a GOES R Solar Imaging Workshop²¹ was held in Boulder, Colorado. This workshop attempted to trace the line from forecaster end user requirements through the relevant science and ultimately suggest a list of measurements. This list was discussed and prioritized into three categories in an open discussion among all participants (Table 2). Only the high priority measurements were considered for additional investigation. Note that the workshop found that the forecast benefits due to combined SXI and coronagraph measurements were much greater than twice the benefits of having either measurement by itself. Workshop participants assumed and encourage the non-imaging solar observations made on the current GOES to continue on GOES R.

Table 2: ROES R Solar Imaging Observational Priorities

High Priority Measurements	Medium Priority Measurements	Lower Priority Measurements
XUV* Imagery	Line-of-Sight Magnetograms	H α Imagery
Solar Coronagraph Imagery	Hard X-ray Spectrometry	White Light Imagery
		Vector Magnetograms

*The XUV band designation includes soft X-rays and the extreme ultraviolet.

The workshop also called for three specific trade studies to be conducted. The first study was the XUV imager study. It would consider optimization of the spectral bandpass for the SXI follow-on instrument. The second study was the coronagraph study. As a new instrument, a substantial effort would need to be invested in defining the coronagraph. Finally, a deployment study was recommended. This study would consider the reliability and continuity issues associated with deploying the instruments on every other GOES spacecraft versus on every GOES spacecraft. Inputs from the GOES R workshop were used to update the Operational Requirements Document.

Having set the observational requirements, the next step is to assess the technical and programmatic feasibility of meeting those requirements. Fundamental physical constraints are set by the technological state of the art, e.g., estimated full-well capacity (the maximum number of electrons a given pixel can hold) on CCDs available for the development schedule. In addition, engineering constraints are placed on the instrument by the spacecraft resources available, e.g., power, volumetric envelope, pointing. Finally, programmatic constraints due to budget and schedule have an impact on what is feasible. The first in-house design analysis has been conducted for the GOES R SXI by the NASA Goddard Space Flight Center (GSFC) Instrument Synthesis and Analysis Laboratory (ISAL). A similar study will be conducted for the white light coronagraph in the fall of 2002.

2.3 Solar X-ray Imager Observational Requirements

The requirements for the SXI follow-on instrument are rather mature because they represent evolution of an existing instrument. These requirements are described as ‘threshold’ and ‘objective.’ Threshold indicates the minimum observational improvement that would result in a substantial improvement in forecasting. Objective indicates the ultimate goal for the requirement. Table 3 summarizes the requirements for the GOES-12, GOES N/O, and GOES R Solar X-ray Imagers.

The observational requirements are broken down into four categories: Response (sensitivity), temperature domain, spatial domain, and temporal domain. Each of these is described in turn. Regarding response, the GOES N/O SXI does not meet requirements for simultaneous flare patrol for short-term radiation storm forecasts and coronal hole location and active region imaging to support mid-term forecasts of geoeffective events. This severe limitation is caused by the relatively small dynamic range of the SXI instrument response when compared to the dynamic range of the observed

solar features. Thus, the top priority requirement for GOES R SXI is to improve system response, particularly the dynamic range. The improved sensitivity will allow better assessment of conditions within coronal holes.

Table 3: Summary of Present and GOES R SXI Requirements.

	GOES 12	GOES N/O	GOES R ²⁰	
			Threshold	Objective
System Response				
Dynamic Range	$\sim 10^2$	$\sim 10^2$	$\sim 10^4$	$\sim 10^7$
Minimum Det. Radiance	7 @ 0.83 nm	85 @ 1.33 nm	42 @ 1.33 nm	42 @ 1.33 nm
(ph-cm ⁻² -arcsec ⁻¹ -sec ⁻¹)*	132 @ 4.47 nm	132 @ 4.47 nm	66 @ 4.47 nm	66 @ 4.47 nm
Effective Temperature				
Range**	1-10 MK	1-10 MK	1-10 MK	0.5-20 MK
Resolution**	10%	10%	10%	5%
Spatial Domain				
Coverage	1.8×10^6 km square†	1.8×10^6 km square†	1.8×10^6 km square†	1.8×10^6 km square†
Resolution	FWHM=5,000 km (Pixel=3,600 km)	FWHM=5,000 km (Pixel=3,600 km)	FWHM=5,000 km (Pixel=1,800 km)	FWHM=3,600 km (Pixel=1,800 km)
Temporal Domain				
Continuity	No gaps > 2 min.	No gaps > 2 min.	No gaps > 2 min.	No gaps > 2 min.
Cadence	1 image per min.	1 image per min.	1 image per min.	1 image per min.

*Minimum detectable radiance is defined nominally for a 0.1 second exposure.

**Full temperature coverage across full dynamic range takes ~12 individual exposures.

†Outer boundary of 1.34 to 1.89 R_{SUN}.

Important features range from 0.5 – 20 MK and include coronal holes, active regions, and flares. It is necessary to distinguish these features by temperature, including flares and the lower corona, in a timely fashion. The GOES N/O SXI can cover the complete temperature regime with maximum fidelity with a set of approximately six (long-short exposure) pairs of images. Reduced temperature coverage can be obtained using three pairs of images. Photospheric and chromospheric emissions are negligible at these temperatures so the corona can be imaged on the solar disk. Ratios of filtered images allow determinations of effective temperature to be made with 10% accuracy. Since features are highly dynamic on the sun, increasing the effective cadence of temperature coverage reduces 'temporal smearing.' With adequate temperature resolution, isothermal plasma models¹ can be used to estimate column density.

The SXI must provide adequate spatial coverage and resolution to distinguish solar features with potential geospace impacts. Since geoeffective activity can take place anywhere on the sun, the entire corona, both on and off disk, must be regularly imaged (0 to > 1.3R_{SUN}). An area of particular interest is the detection of active regions beyond the eastern limb. Monitoring for these regions gives 3-day advance warning of changes in the solar EUV radiance which impacts satellite drag and communications through changes to neutral and ion densities in the thermosphere/ionosphere. Another area of interest is the detection of flares beyond the western limb. Flares in this region can generate relativistic particle events affecting satellites. In addition, the SXI must have the ability to accurately resolve the boundaries of coronal holes and active regions. The GOES N/O resolution and pixel size is sufficient to image compact flares with length scales of $\sim 10,000$ km²². The GOES N/O SXI has pixels which under-sample the mirror point spread function so that the true optical performance is not realized. Decreasing the pixel size to 2.5 arcseconds would meet the Nyquist sampling criterion.

Many events on the Sun take place very rapidly. EIT waves and other eruptive phenomena can have speeds of 100-1000 km/sec. At the high end of this speed range, propagating features cross one 5 arc second pixel in 4 seconds and can cover ~ 0.1 R_{SUN} in the one minute interval between nominal cadence images. In addition, geoeffective events, e.g., proton storms, can take place in as little as 15 minutes after a solar event is detected. Thus, if a set of images taken with different filters or different exposures is to be combined for assessing temperature or creating a wide dynamic range image, it is desirable to complete the image set in 4 seconds. To minimally capture flare initiation or determine the speeds of dynamic features, at least one image set per minute is needed. No interruptions in observation longer than two minutes should be planned.

2.4 Solar Coronagraph Observational Requirements

As a newly proposed instrument, requirements for the GOES coronagraph are less fully developed than those for the follow-on SXI. However, examining the observational requirements and the long history of space-based research coronagraphs, a set of initial requirements can be drawn. These requirements are not yet refined into the 'threshold' and 'objective' categories that exist for the SXI. Table 4 summarizes the requirements for the GOES R coronagraph and similar research instruments.

Table 4: Summary of White Light Coronagraph Requirements vs. Existing and Planned Instruments.

	SOHO LASCO C3 ²³	STEREO SECCHI COR 2 ²⁴	GOES R Requirement ^{21, 25}
System Response			
Dynamic Range	~16,000*	~16000*	$>10^3$ (TBD by study)
Stray Light Level	$1 \times 10^{-12} B_{\text{SUN}}$	$1 \times 10^{-11} B_{\text{SUN}}$	$\sim 3 \times 10^{-12} B_{\text{SUN}}$ (TBD by study)
Spatial Domain			
Coverage	$3.7 - 32 R_{\text{SUN}}$	$2-15 R_{\text{SUN}}$	$2-4$ to $15-30 R_{\text{SUN}}$
Resolution	Pixel=56.0"	Pixel=14"	Pixel<50"
Temporal Domain			
Continuity	-	-	No gaps > 30 min.
Cadence	~1 image per 60 minutes	1 pB set per 20 minutes	>1 image** per 15 min.

*With 14 bit digitization.

**Requirement for color and/or polarization separation of F and K corona is TBD by study.

In broad terms, a GOES coronagraph must be able to detect Earth-directed CMEs. These CMEs often appear as complete or partial halos around the Sun. Detection of so-called partial halo CMEs is important because they may intersect Earth or pass close enough to influence Earth's space environment. The coronagraph must provide images suitable to infer the speed and direction of a halo CME if we are to predict the arrival time at Earth. To do this, it should have sufficient sensitivity, a large enough field of view (FOV) with fine enough spatial resolution, and adequate sampling cadence.

For instrument sensitivity, the key issue is the requirement is to be able distinguish coronal mass ejections from the quiet corona. Figure 1 illustrates the components of the coronal emission. The K-corona is the "true" corona, visible in white light by Thomson scattering of photospheric radiation by coronal electrons. The F-corona is emission is photospheric radiation scattering off dust. The E-corona is the emission-line corona. It is much fainter than the K- or F- contributions, and is seen at specific wavelengths. Since the F-corona contribution dominates beyond about $3 R_{\text{SUN}}$, it is necessary to find means to subtract this contribution from the imaged scene. Several techniques are available that take advantage of the polarization and color differences between the K and F coronal emissions.

The necessary spatial coverage is closely coupled with image cadence. The goal is to be able to obtain at least three images of a given CME feature as it transits the field-of-view. The inner imaging radius is set both by the need to avoid the challenges involved with imaging very close to the Sun's disk and by the desire to image a CME after most of its acceleration has taken place²⁶. The outer edge of the FOV is set, principally, by the sensitivity and dynamic range of the instrument.

The frequency of observations is governed by the need to obtain at least three images of CME features as they transit the field-of-view. Three images ensure that not only can plane-of-sky speed be measured, but also acceleration may be detected. A very fast CME, say 2500 km-s^{-1} , transits time from 4 to $17 R_{\text{SUN}}$ in about 60 minutes. Thus, to ensure that the CME front appears on three exposures, a cadence of 15 minutes is recommended. No gaps of more than 30 minutes should occur.

Further detailed study is recommended for refining the requirements for a space weather operational coronagraph. In addition to refining requirements of response, FOV and resolution, and cadence, a study must include what bandpass and filtering would be best for an operational coronagraph as well as the need for polarization brightness (pB) measurements.

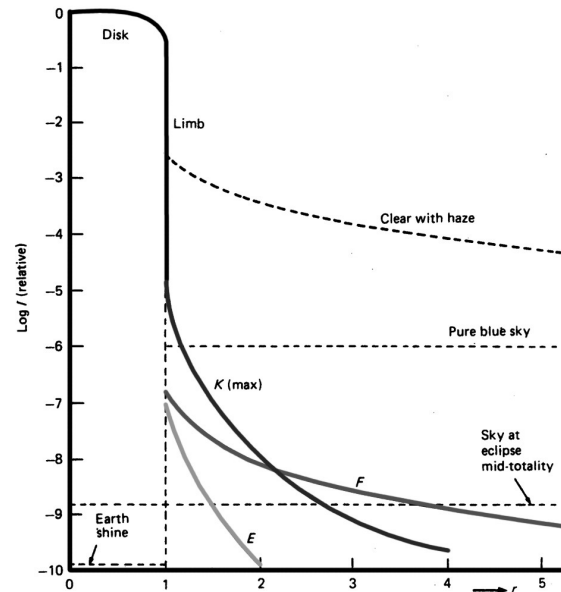


Figure 1: Surface brightness of the observed corona [from ref. 25].

3. GENERAL SPACECRAFT CONCEPTS

The primary mission of the GOES spacecraft is to obtain meteorological observations of Earth²⁷. The baseline constellation consists of two operational satellites and one satellite stored on-orbit. (Alternative multi-platform / dedicated platform constellation configurations are being studied.) The operational satellites are deployed in a geosynchronous orbit $6.6 R_E$ from Earth's center at 75 deg and 135 deg West longitudes. The Earth Imager and Sounder are the primary instruments. Call-up of the stored satellite is dependent on a loss of meteorological data from these instruments. In addition to the meteorological instruments, GOES is equipped with the Space Environment Monitor (SEM), composed of particle sensors, magnetometers, X-ray sensors, and a Solar X-ray Imager. Starting with GOES N/O, a disk integrated solar EUV sensor will be included. Upgrades to the GOES spacecraft can occur with each 'block' change, where a block is a procurement of typically 3-5 spacecraft.

The GOES orbit provides nearly continuous solar viewing, with daily data drop-outs of <90 minutes during two 40-day eclipse seasons each year. If both operational spacecraft are equipped with identical solar instruments, eclipse periods for one spacecraft will be covered by the other spacecraft.

Each GOES spacecraft is three-axis stabilized to its nadir; the SXI and other solar instruments are mounted on the yoke of the solar array panel (Figure 4). An independent north-south pointing platform corrects for seasonal variations in the solar array pointing. During GOES 12 checkout solar array pointing errors of ± 3 arc minutes have been achieved over a period of 24 hours. GOES N/O has pointing step sizes of 52 arc seconds along the N-S axis and 24 arc seconds along the E-W axis. On the GOES 12 and N/O spacecraft, the stepping of the solar array is paused during SXI exposures. Since the spacecraft rotates to maintain nadir pointing, image motion across the detector during an exposure must be compensated. This has been done by electronically advancing detector array lines at the proper rate. In addition, the solar array particularly, and the spacecraft in general, are susceptible to jitter. This dynamic excitation of structural modes occurs when mechanisms on the spacecraft move, the largest of which is the solar array. This has led to the development of on-chip Image Motion Compensation (IMC) for the GOES N/O SXI, but in the E-W direction only.

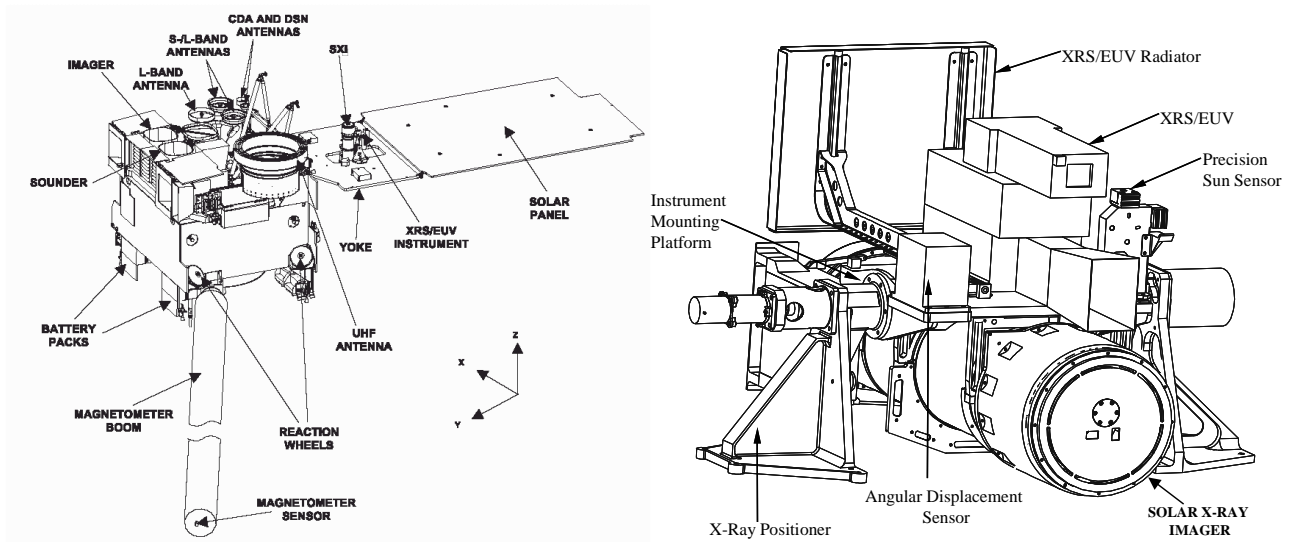


Figure 2: GOES N/O spacecraft and SXI with mounting platform²⁸.

4. X-RAY IMAGER

The GOES R Solar X-ray Imager will represent an evolution of the operational instruments. Thus, first we discuss the current instruments – the GOES 12 prototype that is currently stored on-orbit, and the GOES N/O instruments. Then we present the first draft of a concept instrument for GOES R.

4.1 Current Instruments

The GOES 12 and GOES N/O instruments share many basic features. Each uses monolithic, two-reflection, grazing incidence optics to support a bandpass of roughly 6 to 60 Å. Each has metallic thin-film entrance filters for rejection of IR-Visible-UV solar radiation. A High Accuracy Sun Sensor (HASS) integrated into the instrument provides pointing knowledge. An illumination source is included for detector "aliveness" verification. Both use 512×512 pixel array detectors, though they are of quite different designs. The instruments are operated at basic one minute image cadences using tables stored in on-board memory. Specifications for both instruments are outlined in Table 5. Figure 3 compares the spectral response and sensitivity of current SXIs and research instruments.

The SXI currently flying on the GOES 12 spacecraft was built by NASA's Marshall Space Flight Center (MSFC) with funding from the US Air Force^{27, 29, 30}. It uses a classic Wolter I grazing incidence optical design with a nickel-coated, monolithic Zerodur mirror³¹. The detector is an intensified CCD^{32, 33}. It consists of a Micro Channel Plate (MCP) which acts like an array of photomultiplier tubes with a gain of $\sim 10^3$. The resulting electron clouds impact a phosphor plate which emits at visible wavelengths. The phosphor is optically linked via a Fiber Optic Taper (FOT) to a CCD. The rationale for using the MCP included: very good visible light rejection, very good long-wave sensitivity, and the uncertainty associated with X-ray sensitive CCDs at the time of design. Operational control of imaging sequences is driven by a set of on-board tables that can be modified by ground command³⁴.

The GOES 12 SXI completed Post-Launch Testing (PLT) in 20 December 2001 and demonstrated great success in meeting the primary objectives for solar imaging (minus those fulfilled by a coronagraph)³⁵. On orbit performance has been mostly consistent with that expected from ground testing. The instrument's spatial resolution does not meet original requirements, however ground data processing will likely be able to overcome these shortcomings. Note that the most current SXI data and calibration information is available at <http://www.sec.noaa.gov/sxi/>.

Table 5: Comparison of Present SXI (as built) Specifications and Draft GOES R SXI Specifications.

	GOES 12	GOES N/O	Strawman GOES R
Entrance Filters	AlTi on polyimide	AlTi on polyimide	TBD by Study
Mirror			
Prescription	Wolter I	Hyperboloid – Hyperboloid	Hyperboloid – Hyperboloid
Coating	Nickel	Uncoated	Uncoated
On-axis FWHM	~10 arc sec	6 arc sec	6 arc sec
Off-axis (18') FWHM	~20 arc sec	~11 arc sec	~11 arc sec
Pointing			
HASS Sampling	3.9 arc second	1.6 arc second	TBD by study
E-W	CCD Line advance	CCD Line advance or IMC	CCD Line advance or IMC
N-S	No	No	Piezo IMC
Sampling	16 ms	16 ms	TBD by study
Aliveness source	UV bulb	Blue LED	Blue LED
Analysis Filters			
Mechanism(s)	Single 12 position wheel	Dual six position wheels	TBD by study
Types	'Open', AlTi Poly, Be	AlTi, Al, Sn, Be	TBD by study
Shutter	Electronic	Mechanical	Mechanical
Detector			
Type	MCP/FOT/CCD	CCD*	CCD*
Active Area	512×512 pixels	512×512 pixels	1024×1024 pixels
Pixel Size	5×5 arcsec	5×5 arcsec	2.5×2.5 arcsec
Cooling	Passive (-25°C)	Passive (-35°C)	Active TEC (-70°C)
Control			
Method	Memory Tables	Memory Tables	Memory Tables
Cadence	1-1.5 image/minute	1-1.5 image/minute	1 image set/minute**
Mass (total):	23	27	33
Telescope Assembly	15	14	-
Electronics Boxes	8	13	-
Power			
Peak	57	80	97
Average	42	60	-
Telescope Envelope (cm)†			
Length	76	79	-
Diameter	27	25	-
Telemetry Rate (kbps)	100	100	3,200**

*The CCD is a thinned, back-illuminated, anti-blooming design.

**One 'image set' is considered here to be four image triples covering four spectral bands. The data rate assumes that all the individual images are downlinked each minute with 10% overhead. Significant savings in bandwidth could be achieved with a minimal degree of processing on the instrument.

†Dimensions of the GOES R telescope should be similar the GOES N/O SXI.

A new version of the SXI, built by Lockheed, will be launched on GOES N/O series spacecraft starting in 2004 (Figure 4). There are three primary differences between the GOES 12 and GOES N/O instruments. First, the mirror prescription was changed from a Wolter I design to an optimized hyperboloid-hyperboloid design³⁶. This design provided greater uniformity in spatial resolution than the Wolter I over the relatively large field-of-view. Ground testing showed that the engineering model mirror substantially exceeded requirements³⁷, and it was ultimately selected for the first flight model instrument. The mirror was left uncoated to compensate for the high short wavelength response of the detector.

The second major difference in the instruments is that the GOES N/O series uses a thinned, back-illuminated, X-ray sensitive, anti-blooming CCD. The detector has much higher quantum efficiency than the MCP stack used in the GOES

12 SXI. The CCD functions as an energy integrating detector such that photons of higher energy / shorter wavelength produce more signal than those of lower energy / longer wavelength. This emphasizes shortwave response, as opposed to the GOES 12 detector stack which had uniform response across photon energies. The use of a CCD for directly detecting X-rays necessitates the use of a mechanical shutter instead of the electronic shuttering used for the MCP detector. Overall system-level response was tested and found to exceed requirements by factors of 1.5-10 depending on wavelength.

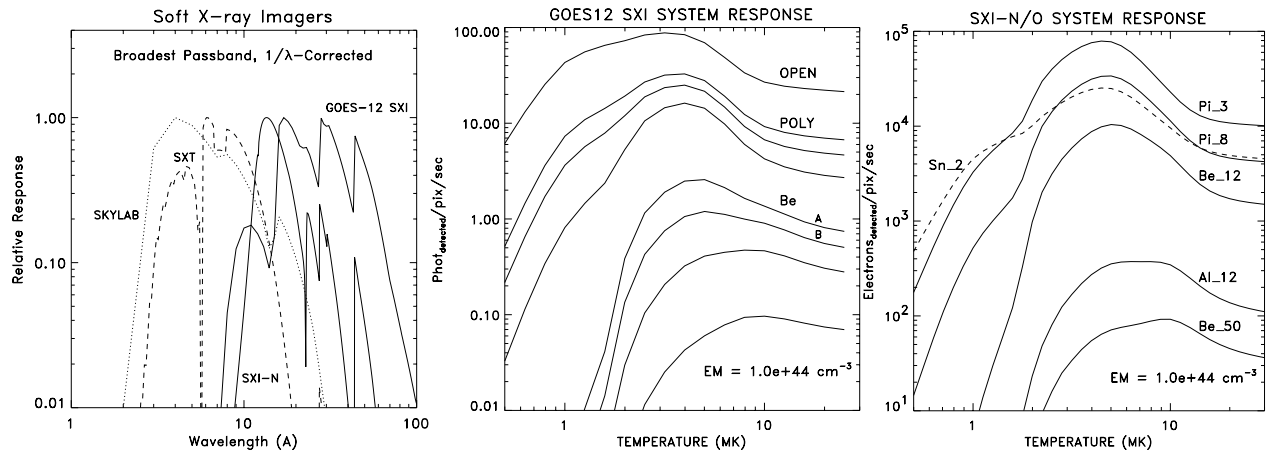


Figure 3: Left to right, GOES 12 and N/O SXI spectral responses compared to those of Skylab S-054 and *Yohkoh* SXT; GOES 12 response to isothermal plasma with a column emission measure of $\sim 10^{27} \text{ cm}^{-5}$; GOES N/O response to an isothermal plasma with a column emission measure of 10^{27} cm^{-5} .

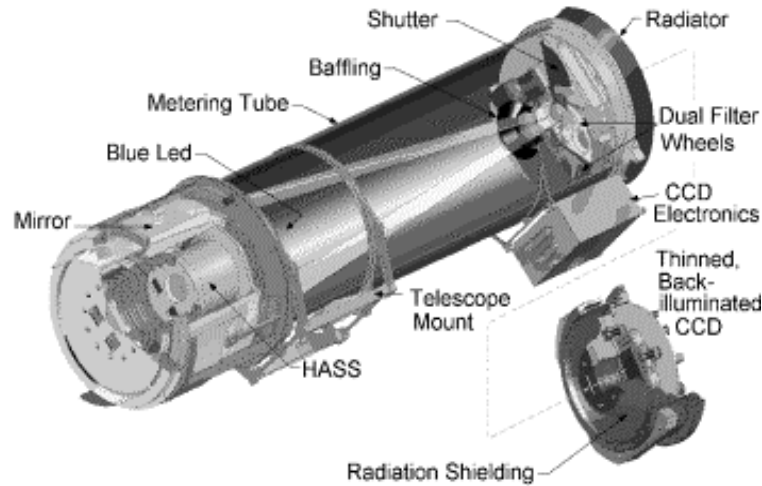


Figure 4: GOES N SXI Schematic

The final difference between the GOES N/O and GOES 12 instruments is really a set of improvements to the system software and control. The fixed-rate line advance to compensate spacecraft geosynchronous rotation has been replaced with an active Image Motion Control system which compensates for E-W jitter using HASS data as input. In addition, the instrument has the capability to interleave additional images and to respond to solar flares and other events autonomously.

4.2 GOES R Concept Instrument

The initial design study by the NASA GSFC Instrument Synthesis and Analysis Laboratory team was completed in July 2002. This team looked at the ability of current technology to meet performance requirements in the context of spacecraft constraints levied on the instrument. Specifically, the team looked at mass, power, volume and telemetry resources and thermal, electrical, and mechanical issues. Overall, the assessment found that the dynamic range improvement from $\sim 10^2$ to $\sim 10^4$ was achievable along with doubling the system sensitivity, and improving resolution by halving the pixel size. The ISAL recommendation was to provide these incremental improvements to the current (N/O) SXI design while maintaining the overall optical design.

To achieve the necessary dynamic range, the ISAL recommended taking three images in each filter position. Each image would be roughly a factor of 10-100 shorter than the previous one. For example, a 10 second exposure would be followed by a 0.4 second exposure which would be followed by a 0.016 second exposure. With this factor of 25 between exposure durations, an image 'triple' would cover a dynamic range of $>10^4$. Because the study recommends continued use of a CCD detector, dynamic range will remain wavelength dependent. Though the ISAL recommended processing these image triples on the ground, selective downlinking of data based on on-board saturated pixel detection would substantially reduce the telemetry bandwidth needed. Pixels that are saturated during long exposures would be replaced by those from shorter exposures and tagged with one of two extra bits. This would result in effectively one 14 bit deep image per triple exposure as opposed to three 12 bit images per triple exposure to be downlinked. Of course, the on-board approach may levy more stringent pointing requirements on the spacecraft and would certainly take more instrument computing power. The ISAL considered a full image set to be taken each minute to consist of four image triples, one for each of four primary filters.

To accommodate the improvement in spatial sampling, the ISAL team recommended a 1024×1024 pixel array with 8 micron pixels. However, substantial investigation on the effects of pixel size reduction on a broad range CCD properties remains to be done. One of these effects would be to reduce the full-well by a factor of four, from about 150,000 to about 40,000. This has an impact on the dynamic range and the desire to increase the sensitivity by a factor of two. Since CCD signal level depends on wavelength of the incident radiation, for the spectral band of 1-6 nm, the photon full-well will range from about 90 to about 550 photons. With dynamic range being defined as full-well signal divided by the signal needed for $\text{SNR}=3$ (9 photons), then the single exposure dynamic range is limited to 10 to 60. Thus, for longer wavelengths the effective dynamic range of 10^4 is easily achievable with three exposures. For shorter wavelengths, the threshold dynamic range can only be achieved with additional exposures.

Part of the improvement in minimum detectable radiance has effectively been achieved through the superior sensitivity of the GOES N/O SXI. Further improvement to meet the requirement with 8 micron pixels may be achieved through filter design or through relaxing the requirement on achieving this sensitivity within 100 ms.

Potential additional improvements for the GOES R SXI include adding piezoelectric N-S guidance to the focal plane based on High Accuracy Sun Sensor (HASS) inputs. This would help reduce jitter which will become a dominant source of blurring with 2.5 arc second pixels. Finally, to reduce radiation damage to the CCD, it was recommended that active thermoelectric cooling be considered to hold the CCD at -70°C .

5. WHITE LIGHT CORONAGRAPH

The initial design study for the coronagraph under consideration for GOES R will occur in the fall of 2002. Thus, only a sketch of one possible design is given at this point. The system would draw on the experience of both the C3 coronagraph on the SOHO spacecraft and the COR 2 coronagraph on the STEREO spacecraft. These instruments are externally occulted and use refractive optics. The basic optical layout for an externally occulted coronagraph is shown in Figure 5. The principle advantages of external versus internal occultation are that stray light and heat rejection are better, since the solar disk is blocked from illuminating the aperture. The principal disadvantage is that spatial resolution decreases dramatically as the inner boundary of the field-of-view is approached, due to vignetting by the occulting disk.

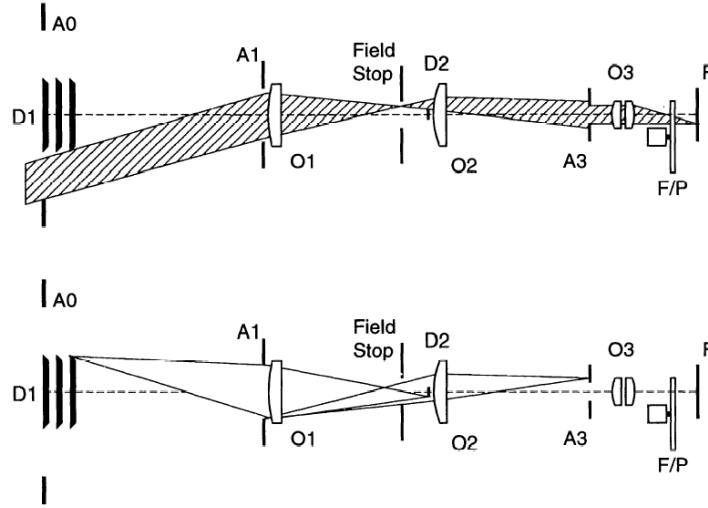


Figure 5: Optical layout for an externally occulted Lyot coronagraph [from ref. 38]: from aperture A0, external occulter D1, entrance aperture A1, objective lens O1, internal occulter D2, field lens O2, Lyot stop A3, relay lens with Lyot spot O3, filter/polarizer wheels F/P, and focal plane F.

Table 6: Comparison of Research Coronagraph Specifications with those of a Possible GOES R Instrument*.

	LASCO C3	COR 2	Strawman GOES R
Optics	Externally Occulted Lyot	Externally Occulted Lyot	Externally Occulted Lyot
Pointing			
Absolute	-	30 arc seconds	TBD by study
Pointing Stability	-	1.5 arc sec during pB sequence	TBD by study
Analysis Optics			
Filters	Broadband, H α , IR	Broadband	TBD by study
Polarizers	Fixed at 0, ± 60 deg.	Rotating half-wave plate	TBD by study
Detector			
Type	CCD	CCD	CCD
Active Area	1024 \times 1024 pixels	2048 \times 2048 pixels	2048 \times 2048 pixels
Pixel Size	56 \times 56 arcsec	14 \times 14 arcsec	17 \times 17 arcsec
Digitization	14 bit	14 bit	14 bit
Cadence	1 image per 60 minutes	1 pB set per 20 minutes	1 pB set per 15 minutes
Telescope Envelope (cm)			
Length	89	135	~ 100
Diameter	11	13	-
Telemetry Rate (kbps)**	4	48	65

*Instrument mass and power are not described because: 1) Previous instruments have been integrated into multi-instrument suites so individual mass and power specifications are difficult to establish, 2) The GOES R coronagraph lacks sufficient maturity.

**Telemetry rate shown is for uncompressed data.

6. SUMMARY AND CONCLUSIONS

The instruments described here would provide dramatic improvements to operational space weather specification and forecasting. In addition, they will continue the historical record of soft X-ray imaging of the Sun, begun by *Yohkoh*'s SXT and extended by the current GOES SXI (in on-orbit storage until called into operations no later than Summer

2003). The possible addition of a coronagraph will be invaluable in detecting and tracking Earthbound coronal mass ejections.

This paper describes NOAA's high-level observational requirements for solar imaging on GOES R. Relevant solar activity is described and, where possible, quantified. The current process of taking the observational requirements and turning them into instrument requirements and specifications is outlined. Specific instrument requirements, as they stand now, for both a follow-on Solar X-ray Imager and new white light coronagraph, are given. Some of the engineering constraints imposed by the baseline spacecraft bus are presented. Finally, the instruments under consideration by NOAA for GOES R, an SXI and a coronagraph, are briefly described.

The requirements process is just beginning, and the launch of GOES R is a decade away. The requirements and specifications for the instruments under consideration will evolve, of course, according to programmatic parameters and technical capabilities. However, the initial sketches drawn here point to substantial improvements that are possible for continuous synoptic monitoring of the Sun. In addition to operations, these observations will provide invaluable context for future solar research observations.

ACKNOWLEDGEMENTS

The authors wish to thank the many contributors to both the current SXI program and the preparation for GOES R solar imaging. These include S. Kirkner, G. Dittberner, and P. Mulligan at NOAA/NESDIS; S. Cauffman, J. Bajpayee, and the ISAL Team at NASA/GSFC; F. Eparvier at the University of Colorado, J. Burkipple at High Altitude Observatory, O. C. St. Cyr at Catholic University of America, the GOES 12 SXI team at NASA/MSFC, the GOES N/O SXI team at NASA/GSFC and LMSAL, and NOAA's space weather partners in the U.S. Air Force. The authors also wish to thank W. Neupert, H. Singer, and E. Hildner at NOAA/SEC and R. Hooker at NOAA/NESDIS for their helpful comments on this paper during its preparation.

REFERENCES

1. Mewe, R., E.H.B.M. Gronenschild, and G.H.J.v.d. Oord, *Calculated X-radiation from Optically Thin Plasmas* V. Astronomy and Astrophysics Supplement Series, 1985. **62**: p. 197-254.
2. Batchelor, D., *Quasi-Stereoscopic Imaging of the Solar X-ray Corona*. Solar Physics, 1994. **155**: p. 57-61.
3. Aschwanden, M.J., et al., *Three-dimensional Stereoscopic Analysis of Solar Active Region Loops. I. SOHO/EIT Observations at Temperatures of $(1.0-1.5) \times 10^6$ K*. The Astrophysical Journal, 1999. **515**(2): p. 842-867.
4. Aschwanden, M.J., et al., *Three-dimensional Stereoscopic Analysis of Solar Active Region Loops. II. SOHO/EIT Observations at Temperatures of 1.5-2.5 MK*. The Astrophysical Journal, 2000. **531**(2): p. 1129-1149.
5. Foley, C.H., J.L. Culhane, and L.W. Acton, *Yohkoh Soft X-ray Determination of Plasma Parameters in a Polar Coronal Hole*. The Astrophysical Journal, 1997. **491**: p. 933.
6. Hara, H., et al., *Temperatures of coronal holes observed with the Yohkoh SXT*. PASJ, 1994. **46**: p. 496.
7. Doschek, G.A., et al., *Properties of Solar Polar Coronal Hole Plasmas Observed above the Limb*. The Astrophysical Journal, 2001. **546**(1): p. 559-568.
8. Geiss, J., et al., *The Southern High-Speed Stream: Results from the SWICS Instrument on Ulysses*. Science, 1995. **268**: p. 1033-1036.
9. Denton, R.E., U. Feldman, *The Relation of Electron Temperature to Emission Measure and Limits of Increase in Emission Measure in Soft X-ray Flares*. The Astrophysical Journal, 1984. **286**: p. 359-362.
10. Tsuneta, S., et al., *The Soft X-ray Telescope for the Solar-A Mission*. Solar Physics, 1991. **136**: p. 37-67.
11. Falconer, D.A., R.L. Moore, and G.A. Gary, *Correlation of the Coronal Mass Ejection Productivity of Solar Active Regions with Measures of Their Global Nonpotentiality from Vector Magnetograms: Baseline Results*. The Astrophysical Journal, 2002. **569**(2): p. 1016-1025.
12. Canfield, R.C., H.S. Hudson, and D.E. McKenzie, *Sigmoidal Morphology and Eruptive Solar Activity*. Geophysical Research Letters, 1999. **26**(6): p. 627.
13. Waljeski, K., et al., *The Composition of a Coronal Active Region*. The Astrophysical Journal, 1994. **429**: p. 909-923.

14. Mason, H.E., et al., *Electron Density and Temperature Structure of Two Limb Active Regions Observed by SOHO-CDS*. Solar Physics, 1999. **189**: p. 129-146.
15. Zarro, D.M., et al., *SOHO EIT Observations of Extreme-Ultraviolet "Dimming" Associated with a Halo Coronal Mass Ejection*. The Astrophysical Journal, 1999. **520**(2): p. L139-L142.
16. Sterling, A.C. and H.S. Hudson, *YOHKOH SXT Observations of X-Ray "Dimming" Associated with a Halo Coronal Mass Ejection*. Astrophysical Journal Letters, 1997. **491**: p. L55-L58.
17. Sime, D.G. and A.J. Hundhausen, *The Coronal Mass Ejection of July 6, 1980: A Candidate for Interpretation as a Coronal Shock Wave*. Journal of Geophysical Research, 1987. **92**(A2): p. 1049-1055.
18. Hildner, E., et al., *The Large Coronal Transient of 10 June 1973*. Solar Physics, 1975. **42**: p. 163-177.
19. St. Cyr, O.C., et al., *Properties of Coronal Mass Ejections: SOHO LASCO Observations from January 1996 to June 1998*. Journal of Geophysical Research, 2000. **105**(A8): p. 18,169-18,185.
20. Singer, H.J., et al., *Space Environment Monitor (SEM) for the Geostationary Operational Environmental Satellites (GOES R+): Operational Requirements Document*. 2002, NOAA Space Environment Center: Boulder, Colorado. p. 27.
21. Eparvier, F.C., *Solar Imaging Needs for the Space Environment Monitor on the Geostationary Operational Environmental Satellites (GOES R+): A Report of the GOES R Solar Imager Workshop*. 2002, University of Colorado, Laboratory for Atmospheric and Space Physics: Boulder, Colorado. p. 30.
22. Garcia, H.A., *Reconstructing the Thermal and Spatial Form of a Solar Flare from Scaling Laws and Soft X-ray Measurements*. The Astrophysical Journal, 1998. **504**: p. 1051-1066.
23. Howard, R.A., et al., *Observations of CMEs from SOHO/LASCO*, in *Coronal Mass Ejections*, N. Crooker, J.A. Joselyn, and J. Feynman, Editors. 1997, American Geophysical Union: Washington, D.C. p. 299.
24. Howard, R.A., J.D. Moses, and D.G. Socker. *Sun-Earth connection coronal and heliospheric investigation (SECCHI)*. in *Instrumentation for UV/EUV Astronomy and Solar Missions*. 2000: SPIE.
25. St. Cyr, O.C. *Experience with Spaceborne Coronagraphs*. in *GOES R Solar Imaging Workshop*. 2001. Boulder, Colorado.
26. Zhang, J., et al., *On the Temporal Relationship Between Coronal Mass Ejections and Flares*. The Astrophysical Journal, 2001. **559**: p. 452-462.
27. *GOES I-M Data Book*. 1996, NASA Goddard Space Flight Center: Greenbelt, MD. p. 196.
28. *GOES NO/P/Q - The Next Generation*. 2001, NASA Goddard Space Flight Center. p. 36.
29. Davis, J., D. Bagdigian, S. Buschmann, K. Russell, and K. Wallace. *The Solar X-ray Imager for the Geostationary Operational Environmental Satellite (GOES)*,. in *AIAA Space Programs and Technologies Conference*. 1994. Huntsville, AL, USA.
30. Bornmann, P.L., et al. *The GOES Solar X-ray Imager: Overview and Operational Goals*. in *GOES-8 and Beyond, Proc. SPIE Vol. 2812*. 1996.
31. Smithers, M.E. and D.E. Zissa, *Solar X-ray Imager (SXI) Optical Performance Analysis*. SPIE, 1996. **2805**: p. 115-120.
32. Corder, E.L., *Development of the Solar X-ray Imager (SXI) Camera*. SPIE, 1994. **2214**: p. 294-300.
33. Russell, K., J. Briscoe, E. Corder, S. Wallace, and J. H. Chappell, *The Solar X-ray Imager (SXI) Detector Calibration and Characterization*. SPIE, 1996. **2812**: p. 638-650.
34. Wallace, K.S., T. A. Brown, and K. A. Freestone. *A Table-Driven Control Method to Meet Continuous, Near-Real-Time Observation Requirements for the Solar X-ray Imager*. in *17th Digital Avionics Conference*. 1998. Seattle, Washington.
35. Balch, C.C., et al. *First Forecast Products from The GOES-12 Solar X-ray Imager*. in *82nd AMS Annual Meeting, Sixth Symposium on Integrated Observing Systems*. 2002. Orlando, Florida.
36. Harvey, J.E., P. L. Thompson, and A. Krywonos, *Hyperboloid-Hyperboloid Grazing Incidence X-ray Telescope Designs for Wide-Field Imaging Applications*. SPIE, 2000. **4012**: p. 328-341.
37. Catura, R., et al. *Performance of the engineering model x-ray mirror of the Solar X-ray Imager (SXI) for future GOES missions*. in *X-Ray Optics, Instruments, and Missions IV*. 2000: SPIE.
38. Brueckner, G.E., et al., *The Large Angle Spectroscopic Coronagraph (LASCO)*. Solar Physics, 1995. **162**: p. 357-402.